# The NJL model and the dressed Polyakov Loop

Bachelor-Thesis von Alexander Knetsch
September 2011

TECHNISCHE
UNIVERSITÄT
DARMSTADT

Institut für Kernphysik
Theoretische Kernphysik
AG Prof. Dr. Fischer

The NJL model and the dressed Polyakov Loop

Vorgelegte Bachelor-Thesis von Alexander Knetsch

1. Gutachten: PD. Dr. Buballa
2. Gutachten: Prof. Dr. Fischer

Tag der Einreichung:

**Erklärung zur Bachelor-Thesis**

Hiermit versichere ich, die vorliegende Bachelor-Thesis ohne Hilfe Dritter nur mit den angegebenen Quellen und Hilfsmitteln angefertigt zu haben. Alle Stellen, die aus Quellen entnommen wurden, sind als solche kenntlich gemacht. Diese Arbeit hat in gleicher oder ähnlicher Form noch keiner Prüfungsbehörde vorgelegen.

Darmstadt, den September 13, 2011

(Alexander Knetsch)

## Contents

## 1 Introduction

The Nambu-Jona-Lasinio(NJL) model is an effective quantum field theoretical model to describe the interaction of quark fields. Although it is an effective theory and not renormalizable it is an important tool to explore chiral symmetry breaking, which is an interesting behaviour of quarks. Another interesting behaviour is the confinement. Quarks are never seen alone in experiment. As soon as they exceed a certain energy they can build quark-couples, Mesons. The underlying law is that free particles are supposed to be neutral in colour-charge. A model describing the behaviour of quarks should include confinement, but the NJL-model lacks confinement. A flicker of hope in this case comes from lattice/full QCD. The dressed Polyakov loop is an order parameter for confinement-deconfinement transition. It can be calculated by modifying the chiral condensate to the dual condensate. Even though the NJL model does not include confinement, it is possible to calculate a dressed Polyakov loop since it does include a chiral condensate, which is an order parameter for the chiral symmetry breaking. In this work we will calculate the dressed Polyakov loop for a system with number of colours 3 and the number of flavours 2.

# 2 The theoretical background

## 2.1 The Polyakov Loop in lattice QCD

The Polyakov-Loop is an order parameter for center symmetry breaking and therefore also for confinement-deconfinement crossover [1]. In lattice QCD the 4-dimensional space-time is not continuus but discretely divided into coordinates on a 4-dimensional lattice with a fixed distance $a$ between lattice points:

$$x_\mu \rightarrow an_\mu$$

The space-time also is not infinite. It has a fixed Volume $V$ in a finite space

$$\Gamma = \{n = (n_1, n_2, n_3, n_4) | n_\mu \in [0, N_\mu - 1]\}$$

Usual conventions to achieve that are periodic ($_{\psi(aN_\mu) = \psi(0))}$) or antiperiodic ($_{\psi(aN_\mu) = -\psi(0))}$)boundary conditions. A Wilson Loop is the trace of the path ordered product of gauge transporters $U_\mu(k)$ along a closed loop on the lattice.

$$W = Tr_c\Big[\prod_{(k,\mu)\in\Gamma} U_\mu(k)\Big]$$

A Polyakov-loop $P(\mathbf{n})$ is a Wilson loop, which winds around the complete time direction. The average value of the Polyakov loop is calculated this way:

$$\mathscr{P} = \frac{1}{|\Gamma|}\sum_{n\in\Gamma} P(\mathbf{n}) \tag{2.1}$$

### 2.1.1 The Polyakov Loop and Confinement

The value of the average of the Polyakov loop which is only wrapped around the time direction one time is proportional to the exponential of the free energy of a single quark.

$$< \mathscr{P} > \sim e^{-cF_{quark}} \tag{2.2}$$

with a constant $c$. In a theory including confinement with the Polyakov loop as confinement transition order parameter there is a phase where it is impossible to find a single quark. In this phase, the confined phase, the free energy $F_{quark}$ is infinite and consequently $< \mathscr{P} >= 0$. On the other hand in the deconfined phase, $F_{quark}$ is finite and therefore $< \mathscr{P} > \neq 0$.

## 2.2 The Dressed Polyakov Loop in QCD

The dressed Polyakov Loop is another order parameter for center symmetry [1]. For $m \rightarrow \infty$ it is equal to the thin Polyakov loop, which is the shortest Polyakov loop that winds once around the time direction [1]

## 2.3 History of the NJL-model

In 1961 Y. Nambu and G. Jona-Lasinio suggested in [5] a model for the interactions between nucleons and mesons. The nucleon mass was suggested to arise from a self-energy of the fermion field through a gap-equation mechanism, which was a mechanism already used in BCS theory of superconductivity. It describes a gap between the ground state and the excited state of a superconductor. In analogy to the BCS-theory Nambu and Jona-Lasinio used this mechanism to describe the nucleon mass in a Hartree-Fock approximation. Due to the fact that quarks have not been discovered that time, they considered elementary nucleon fields. Nambu and Jona-Lasinio were aware of the fact, that the model does have a divergent self-energy term. Therefore a phenomenological cut-off parameter $\Lambda$ was introduced. $\Lambda$ as well as a coupling constant are not fundamental and have to be chosen to fit to the experiment. Nowadays the benefits of the NJL model are that it includes or can include certain symmetries which are also important in full QCD, but the calculations are easier and faster in the NJL model.

## 2.4 Properties of the NJL-model

In this work we investigate the two-flavour NJL model ($N_f = 2$). The form of this Lagragian is:

$$\mathscr{L} = \bar{\psi}(i\partial\!\!\!/ - m)\psi + G_s[(\bar{\psi}\psi)^2 + (\bar{\psi} i\gamma_5 \vec{\tau}\psi)^2] \tag{2.3}$$

The first term is the Dirac part for the free quark fields. $m = diag(m_u, m_d)$ is the bare mass-matrix. The other terms are the interactions, where $\tau^k$ $(k = 1,2,3)$ are the isospin Pauli matrices, $G$ is the coupling constant and $\gamma_5 = i\gamma_0\gamma_1\gamma_2\gamma_3$. The masses of the up and the down quark are similar, thus in this work we use only one value $m = m_u = m_d$. Unfortunately the NJL model lacks the feature of confinement. The NJL model is not renormalizable but it does have a divergent self-energy term. Therefore we have to regularize it. In this work we will use a three-momentum cut-off $\Lambda$, which breaks the Lorentz covariance, but maintains the chiral symmetry [2].

### 2.4.1 U(1)-Symmetry

The used Lagrangian is invariant under a global transformation

$$\psi \to e^{-i\alpha}\psi, \ \alpha \in \mathbb{R} \tag{2.4}$$

This leads to the conservation of the baryon number which is an important feature of the strong interaction.

### 2.4.2 SU(2)-Symmetry

$\mathscr{L}$ is also invariant under an $SU(2)_V$ transformation, which is a rotation in isospin-space

$$\psi \to e^{-i\vec{\tau}\frac{\vec{\theta}}{2}}\psi, \vec{\theta} \in \mathbb{R}^3 \tag{2.5}$$

For $m = 0$ $\mathscr{L}$ is also invariant under an $SU(2)_A$ transformation:

$$\psi \to e^{-i\gamma_5\vec{\tau}\frac{\vec{\theta}}{2}}\psi \ , \vec{\theta} \in \mathbb{R}^3 \tag{2.6}$$

These two symmetries together form an interesting one, which is an important feature of the NJL model.

### 2.4.3 Chiral symmetry

An $SU(2)_V \otimes SU(2)_A$ symmetry is called chiral symmetry. Because $SU(2)_A$ is only conserved at $m = 0$ chiral symmetry for small $m$ is only approximatively conserved. The chirality of a massless particle with spin $\pm\frac{1}{2}$ describes whether its spin is aligned or anti-aligned with its momentum. In the chiral limit the chiral symmetry is spontaneously broken at values $(T_c, \mu_c)$. For small bare quark masses the influence of $m$ is of minor importance so that we can speak of a spontaneous symmetry breaking, too. In the NJL model it is possible to explicitly see this spontaneous chiral symmetry breaking by calculating the global minima of thermodynamic potential of a quark field. [2]

### 2.4.4 Dynamical mass generation - The Gap Equation

In modern field theories a particle is no longer seen as a single particle but as a cloud of particles and anti-particles it can transform into. Thus the mass of a single particle is no more as simply defined as in classic mechanics. A feature of the NJL model is the dynamical mass generation which is calculated due to a self-energy term. In this work we first want to linearize the Lagrangian. In order to do so we will do a meanfield approximation (Hartree). $\bar{\psi}\psi$ will be set to be its non zero expectation value $<\bar{\psi}\psi>$ plus a small disturbance $\delta(\bar{\psi}\psi)$.

$$\bar{\psi}\psi = <\bar{\psi}\psi> + \delta(\bar{\psi}\psi) \tag{2.7}$$

For the Lagrangian this means:

$$\mathcal{L} \approx \bar{\psi}(i\partial\!\!\!/ - m)\psi + G_s[<\bar{\psi}\psi>^2 + 2<\bar{\psi}\psi>\delta(\bar{\psi}\psi) + \underbrace{\delta(\bar{\psi}\psi)^2}_{\to 0} + (\bar{\psi}i\gamma_5\tau\psi)^2] \tag{2.8}$$

$\delta(\bar{\psi}\psi)^2$ is small enough to be set zero.
Consequently $(\bar{\psi}i\gamma_5\tau\psi)$ should also be used in meanfield approximation:

$$(\bar{\psi}i\gamma_5\tau\psi) = <\bar{\psi}i\gamma_5\tau\psi> + \delta((\bar{\psi}i\gamma_5\tau\psi))$$

$<\bar{\psi}i\gamma_5\tau\psi>$ could break parity, so is assumed to be zero, like it is done in [2]. Consequently we can state that $(\bar{\psi}i\gamma_5\tau\psi)^2 \approx 0$.
Using also equation (2.7) again $\mathcal{L}$ now transforms to

$$\mathcal{L} \approx \bar{\psi}(i\partial\!\!\!/ - m)\psi + G_s[<\bar{\psi}\psi>^2 - 2<\bar{\psi}\psi>^2 + 2(\bar{\psi}\psi)<\bar{\psi}\psi>] \tag{2.9}$$

Because $<\bar{\psi}\psi>$ and $G_s$ are scalar values, they commute with $\psi$ or $\bar{\psi}$. So we rewrite the Lagrangian in the following way.

$$\mathcal{L} \approx \bar{\psi}(i\partial\!\!\!/ - \underbrace{(m - 2G_s<\bar{\psi}\psi>)}_{M})\psi - G_s<\bar{\psi}\psi>^2 \tag{2.10}$$

We already mentioned that mass does not have to be a simple, fixed expression. We define an effective mass $M$, or with different name, a constituent mass

$$M = m - 2G_s<\bar{\psi}\psi>. \tag{2.11}$$

$<\bar{\psi}\psi>$ is calculated as follows:

$$<\bar{\psi}\psi> = T\sum_n \int \frac{\mathrm{d}^3\mathrm{p}}{(2\pi)^3}\mathbf{Tr}\, S(i\omega_n + \mu, \vec{p}) \tag{2.12}$$

$S(i\omega_n + \mu, \vec{p})$ is the propagator

$$S(i\omega_n + \mu, \vec{p}) = \frac{1}{\gamma_0(i\omega_n + \mu) - \gamma_i p_i - M + i\epsilon} \tag{2.13}$$

and $\omega_n$ are the so called Matsubara frequencies [3]. In the Matsubara theory the time is analytically continued to imaginary values with domain $\tau \in [0, \beta]$ where $\beta = \frac{1}{T}$. In a Fourier series this has the form

$$\psi(\vec{x}, \tau) = \sum_n \psi_n(\vec{x})\, e^{i\omega_n \tau}\ ,\ n\ \in \mathbb{N} \tag{2.14}$$

Furthermore the fields have to obey boundary conditions.
By now we are working with fermionic fields, so we should use the fermionic boundary conditions:

$$\psi(\vec{x}, 0) = -\psi(\vec{x}, \beta) \tag{2.15}$$

Now we write both fields in Fourier series.

$$\sum_n \psi_n(\vec{x}) = -\sum_n \psi_n(\vec{x})\, e^{i\omega_n \beta} \tag{2.16}$$

This means for the Matsubara frequencies:

$$\omega_n = (2n-1)\pi T \tag{2.17}$$

If we had bosonic fields the boundary conditions we would have to require:

$$\psi(\vec{x}, 0) = \psi(\vec{x}, \beta) \tag{2.18}$$

and the corresponding Matsubara frequencies would be

$$\omega_n = 2n\pi T \tag{2.19}$$

Later on we will return to these boundary conditions and generalize them.
Because the propagator $S(i\omega_n + \mu, \vec{p})$ depends on the constituent mass $M$, the chiral condensate $< \bar{\psi}\psi >$ also has this dependence. In order to solve the gap equation (2.11) we have to take this into consideration. The gap equation is not always analytically solvable and can have several solutions. A way to choose usefull solutions, presented in [2], is by calculating the thermodynamic potential.
In case of this work it is reasonable to use the grand canonical potential.

$$\Omega(T, \mu; M) = -\frac{T}{V} lnZ \tag{2.20}$$

with the grand canonical partition function Z. This can be transformed into [2]:

$$\Omega(T, \mu; M) = \frac{(m-M)^2}{4G_s} - T\sum_n \int \frac{\mathrm{d}^3\mathrm{p}}{(2\pi)^3} \mathbf{Tr}\, \ln\Big(\frac{1}{T} S^{-1}(i\omega_n, \vec{p})\Big) + \ const. \tag{2.21}$$

In this work the number of colors is $N_c = 3$ and the number of flavours is $N_f = 2$. Thus we get for the thermodynamic potential:

$$\Omega(T,\mu;M) = \frac{(m-M)^2}{4G_s} - 2N_c N_f \iiint\limits_{\|\vec{p}\|<\Lambda} \frac{\mathrm{d}^3\mathrm{p}}{(2\pi)^3}\left[E + T\ ln(1+e^{-\beta(E-\mu)}) + T\ ln(1+e^{-\beta(E+\mu)})\right] \tag{2.22}$$

It can be proven that

$$<\bar{\psi}\psi> = \frac{\partial\Omega(T,\mu;M)}{\partial m} \tag{2.23}$$

and

$$0 = \frac{\partial\Omega(T,\mu;M)}{\partial M} \tag{2.24}$$

is equivalent to the gap equation (2.11). The extrema of the thermodynamic potential are possible solutions for the gap equations. But only the minima are stable solutions. As additional criterion for $M$ we require that $\Omega(T,\mu;M)$ has at least one minima. In the chiral limit the thermodynamic potential is symmetric around $M = 0$. In this case we select the positive solution.

## 3 Analytical calculations

### 3.1 The $\phi$-dependent Chiral Condensate

As we already pointed out, a proper way to calculate the chiral condensate is the Matsubara-formalism.

$$< \bar{\psi}\psi >= 4\, N_c N_f M T \sum_n \iiint_{\|\vec{p}\|<\Lambda} \frac{\mathrm{d}^3\mathrm{p}}{(2\pi)^3} \frac{1}{(i\omega_n + \mu)^2 - p^2 - m^2} \tag{3.1}$$

with the Matsubara frequencies $\omega_n$ and number of colors $N_c = 3$ and number of flavours $N_f = 2$. $\Lambda = 631.5$ MeV and $G_s = 5.498\ \mathrm{GeV}^{-2}$ are model parameters. We selected the same values as used in [4] to be able to compare the results. We want to generalize the boundary conditions now by adding a phase $\phi \in [0, 2\pi]$ which can continously change the boundary conditions:

$$\psi(\vec{x}, \beta) = e^{-i\phi}\psi(\vec{x}, 0) \tag{3.2}$$

In this way we find a generalized $\phi$-dependent Matsubara frequency:

$$\omega_n(\phi) = (2\pi n - \phi)T, \quad \phi \in [0, 2\pi] \tag{3.3}$$

The already known boundary conditions are then the special cases:

$$\omega_n(\phi = 0) = 2\pi T n \mathrel{\widehat{=}} \text{bosonic boundary conditions} \tag{3.4}$$

$$\omega_n(\phi = \pi) = (2n - 1)\pi T \mathrel{\widehat{=}} \text{fermionic boundary conditions} \tag{3.5}$$

This leads us to a $\phi$- dependent chiral condensate:

$$< \bar{\psi}\psi >_\phi = T \sum_n \int \frac{\mathrm{d}^3\mathrm{p}}{(2\pi)^3} \mathbf{Tr}\, S(i\omega_n(\phi) + \mu, \vec{p}) \tag{3.6}$$

$$= 4\, N_c N_f M T \sum_n \iiint_{\|\vec{p}\|<\Lambda} \frac{\mathrm{d}^3\mathrm{p}}{(2\pi)^3} \frac{1}{(i\omega_n(\phi) + \mu)^2 - p^2 - m^2} \tag{3.7}$$

A rough draft of the poles which are represented by the sum over the Matsubara frequencies and the influence of $\phi$ can be seen in figure (3.1). The basic idea is that the sum over the Matsubara frequencies looks like a sum over residues. Hence, to solve this equation we first use the residue theorem backwards. We identify the sum over the Matsubara frequencies with a line integral over the trajectory $C_1$, which winds around all poles on the imaginary axis.

$$< \bar{\psi}\psi >_\phi = 4\, N_c N_f M T \iiint_{\|\vec{p}\|<\Lambda} \frac{\mathrm{d}^3\mathrm{p}}{(2\pi)^3} \oint_{C_1} \frac{\mathrm{dz}}{i2\pi} n(z) \frac{1}{(\mu + z)^2 - E^2} \frac{1}{Res(z_n)} \tag{3.8}$$

with $n(z) = \frac{1}{e^{\beta z} - e^{-i\phi}}$ , $Res(z_n) = +Te^{i\phi}$ , $\beta = \frac{1}{T}$ and $E = \sqrt{p^2 + M^2}$ .
We can transform the trajectory of $C_1$ equivalently into $C_2$, which are 2 trajectories winding around the 2 poles of the term $\frac{1}{(z+\mu)^2 - E^2}$ : $\{-\mu + E,\ -\mu - E\}$.

$$< \bar{\psi}\psi >_\phi = 4\, N_c N_f M\, e^{-i\phi} \iiint\limits_{\|\vec{p}\|<\Lambda} \frac{\mathrm{d}^3\mathrm{p}}{(2\pi)^3} \oint_{C_2} \frac{\mathrm{dz}}{i2\pi} n(z) \frac{1}{(\mu + z)^2 - E^2} \tag{3.9}$$

Figure (3.1) shows the transformation of the equivalent integration trajectories $C_1 \to C_2$. In the figure on the lhs. the top and bottom part of the trajectory does not contribute value to the integral since it is considered to be infinitesimally small. The arcs in the image in the middle also do not contribute value, because the radius is set to $\infty$. $\phi$ changes the position of the poles. Their number is countable infinite with a fixed distance in $\pm\Im(z)$-direction. Black stands for bosonic boundary conditions and blue for fermionic boundary conditions. In our calculations $\phi$ can have any value in $\mathbb{R}$. Taking into consideration that there is an infinite number of poles on the imaginary axis and because of that the position of the poles repeats in $\phi$ the result of the integral should be periodic in $2\pi$ for fixed $T$.

Figure 3.1: The integration paths $C_1$ and $C_2$ and their transformation into each other.

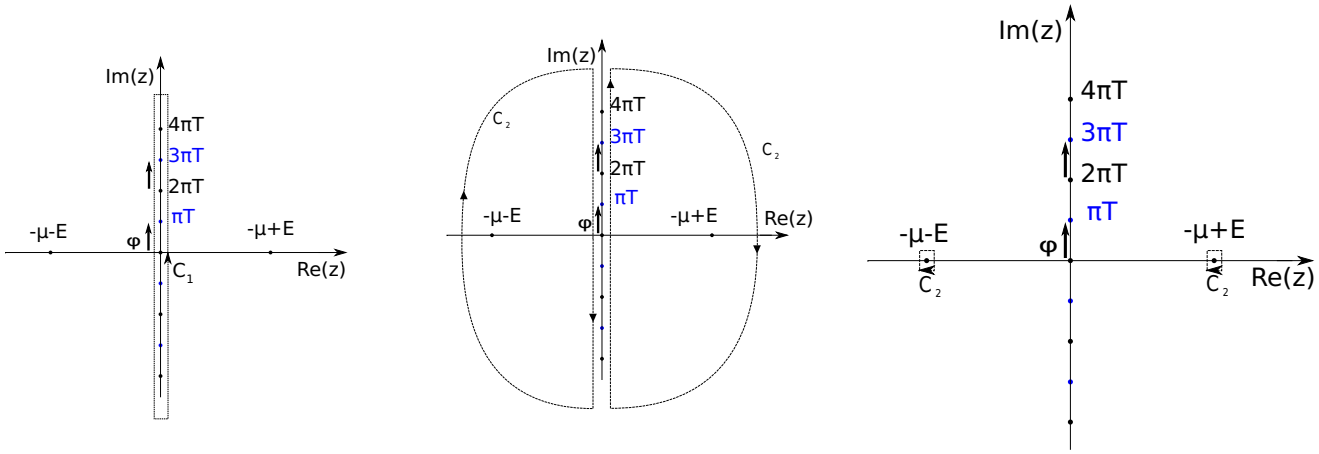


We use the residue theorem one more time.

$$< \bar{\psi}\psi >_\phi = -4\, N_c N_f M \iiint\limits_{\|\vec{p}\|<\Lambda} \frac{\mathrm{d}^3\mathrm{p}}{(2\pi)^3} \left[ \frac{1}{2E} \frac{e^{-i\phi}}{e^{\beta(E-\mu)} - e^{-i\phi}} + \frac{1}{-2E} \frac{e^{-i\phi}}{e^{\beta(-E-\mu)} - e^{-i\phi}} \right] \tag{3.10}$$

$$= -4\, N_c N_f M \iiint\limits_{\|\vec{p}\|<\Lambda} \frac{\mathrm{d}^3\mathrm{p}}{(2\pi)^3} \frac{1}{2E} \left[ \frac{1}{e^{\beta(E-\mu)+i\phi} - 1} - \frac{1}{e^{\beta(-E-\mu)+i\phi} - 1} \right] \tag{3.11}$$

This can be transformed by using the relation $\frac{1}{e^x - 1} = -\frac{1}{e^{-x} - 1} - 1$

$$< \bar{\psi}\psi >_\phi = -4\, N_c N_f M \iiint\limits_{\|\vec{p}\|<\Lambda} \frac{\mathrm{d}^3\mathrm{p}}{(2\pi)^3} \frac{1}{2E} \left[ \frac{1}{e^{\beta(E-\mu)+i\phi} - 1} + \frac{1}{e^{\beta(E+\mu)-i\phi} - 1} + 1 \right] \tag{3.12}$$

The integrand is only $p^2$-dependent. Thus the integral can be transformed into spherical coordinates.

$$< \bar{\psi}\psi >_\phi = -4\, N_c N_f M 4\pi \int_0^\Lambda \frac{\mathrm{dp}}{(2\pi)^3} \frac{p^2}{2E} \left[ \frac{1}{e^{\beta(E-\mu)+i\phi} - 1} + \frac{1}{e^{\beta(E+\mu)-i\phi} - 1} + 1 \right] \tag{3.13}$$

$$< \bar{\psi}\psi >_\phi = -\frac{N_c N_f M}{\pi^2} \int_0^\Lambda \mathrm{dp} \frac{p^2}{E} \left[ \frac{1}{e^{\beta(E-\mu)+i\phi} - 1} + \frac{1}{e^{\beta(E+\mu)-i\phi} - 1} + 1 \right] \tag{3.14}$$

As previously done for equation (2.21) that we can now define the $\phi$-dependent thermodynamic potential analogous to equation (2.22)

$$\Omega_\phi(T,\mu;M) = \frac{(m-M)^2}{4G_s} - 2N_c N_f \iiint\limits_{\|\vec{p}\|<\Lambda} \frac{\mathrm{d^3p}}{(2\pi)^3} \left[ E + T\ ln(1 + e^{-\beta(E-\mu+T(i\phi-i\pi))}) + T\ ln(1 + e^{-\beta(E+\mu-T(i\phi-i\pi))}) \right]$$

This is interesting, because we now do have a $\phi$-dependent potential with an imaginary part $\Im(\Omega_\phi(T,\mu;M)) \neq 0$ for $\phi \neq n\pi$.
We can do a substitution $\tilde{\mu} = \mu - iT(\phi - \pi)$ where $\tilde{\mu}$ is to be seen as kind of a complex chemical potential, which turns to $\mu$ again for fermionic boundary conditions. The $\phi$-dependent chiral condensate after the substitution is:

$$< \bar{\psi}\psi >_\phi = -4\, N_c N_f M 4\pi \int_0^\Lambda \frac{\mathrm{dp}}{(2\pi)^3} \frac{p^2}{2E} \left[ - \frac{1}{e^{\beta(E-\tilde{\mu})} + 1} - \frac{1}{e^{\beta(E+\tilde{\mu})} + 1} + 1 \right] \tag{3.15}$$

and the grand canonical potential turns

$$\Omega_\phi(T,\mu;M) = \frac{(m-M)^2}{4G_s} - 2N_c N_f \iiint\limits_{\|\vec{p}\|<\Lambda} \frac{\mathrm{d^3p}}{(2\pi)^3} \left[ E + T\ ln(1 + e^{-\beta(E-\tilde{\mu})}) + T\ ln(1 + e^{-\beta(E+\tilde{\mu}))}) \right] \tag{3.16}$$

As we can see in eqn. (3.10) the $\phi$-dependent chiral condensate can achieve complex values. We seperate $< \bar{\psi}\psi >_\phi$ into real and imaginary part:

$$\Re(< \bar{\psi}\psi >_\phi) = -\frac{N_c N_f}{\pi^2} M \int_0^\Lambda \mathrm{dp}\ \frac{p^2}{E} \left[ 1 + \frac{e^{\beta(E-\mu)} cos(\phi) - 1}{e^{2\beta(E-\mu)} - 2\, e^{\beta(E-\mu)} cos(\phi) + 1} + \frac{e^{\beta(E+\mu)} cos(\phi) - 1}{e^{2\beta(E+\mu)} - 2\, e^{\beta(E+\mu)} cos(\phi) + 1} \right] \tag{3.17}$$

$$\Im(< \bar{\psi}\psi >_\phi) = +\frac{N_c N_f}{\pi^2} M \int_0^\Lambda \mathrm{dp}\ \frac{p^2}{E} \left[ - \frac{e^{\beta(E-\mu)} sin(\phi)}{e^{2\beta(E-\mu)} - 2\, e^{\beta(E-\mu)} cos(\phi) + 1} + \frac{e^{\beta(E+\mu)} sin(\phi)}{e^{2\beta(E+\mu)} - 2\, e^{\beta(E+\mu)} cos(\phi) + 1} \right] \tag{3.18}$$

We have to note that at this point we assume the bare quark mass $m$ and the constituent mass $M$ to be real, which is a strong approximation to stay close to [4]. This is important, because the gap equation for a complex thermodynamic potential would be

$$\frac{\partial \Re(\Omega_\phi(T,\mu;M))}{\partial M} + \frac{\partial \Im(\Omega_\phi(T,\mu;M))}{\partial M} = 0 \tag{3.19}$$

In consequence the gap equation just needs to be solved in $\mathbb{R}$.

## 3.2 Calculation of the dressed Polyakov loop

The dual quark condensate is defined by a Fourier-integration over the $\phi$-dependent chiral condensate with a dual variable $n$.

$$\Sigma_n = -\frac{1}{2\pi}\int_0^{2\pi} \mathrm{d}\phi \; e^{-in\phi} < \bar{\psi}\psi >_\phi \tag{3.20}$$

For the case of $n = 1$ we get the dressed Polyakov loop.

$$\Sigma_1 = -\frac{1}{2\pi}\int_0^{2\pi} \mathrm{d}\phi \; e^{-i\phi} < \bar{\psi}\psi >_\phi \tag{3.21}$$

In this work the dressed Polyakov loop is calculated in 2 ways. First in the way it is described in [4] and second by taking the imaginary part of the boundary condition dependent chiral condensate into account.

### 3.2.1 Dressed Polyakov loop from real considered $\Omega_\phi(T, \mu; M)$

In [4] only the real part of the $\phi$-dependent thermodynamic potential $\Omega_\phi$ is considered. Hence $< \bar{\psi}\psi >_\phi$ can not have an imaginary part, because it has to fullfill eqn. (2.23). Therefore we get to calculate the dressed Polyakov loop as follows:

$$\Sigma_1 = -\frac{1}{2\pi}\int_0^{2\pi} \mathrm{d}\phi \; \Re(< \bar{\psi}\psi >_\phi)\, cos(\phi) \tag{3.22}$$

### 3.2.2 Dressed Polyakov loop with $\Omega_\phi(T, \mu; M)$ considered to be complex

As we can see from eqn. (3.15), for $\phi \neq n\pi$, $< \bar{\psi}\psi >_\phi$ does have a nonzero imaginary part. In full QCD the potential $\Omega(T, \mu; M)$ can also be complex. Therefore in this work there is a slightly alternatively calculated dressed Polyakov loop additionally presented. We assume $\Omega_\phi$ and therefore also $< \bar{\psi}\psi >_\phi$ to be complex. The constituent quark mass needs to be calculated by solving the gap equation
$0 = M + 2G_s < \bar{\psi}\psi >_\phi - m$ for real $M$ only as we assumed recently. Consequently the masses in the imaginary part of $< \bar{\psi}\psi >_\phi$ are also calculated by solving a real gap equation. The dressed Polyakov loop is still defined like it is in equation (3.21).

$$\Sigma_1' = -\frac{1}{2\pi}\int_0^{2\pi} \mathrm{d}\phi e^{-i\phi} < \bar{\psi}\psi >_\phi$$

$$= -\Big[\frac{1}{2\pi}\int_0^{2\pi} \mathrm{d}\phi \Re(< \bar{\psi}\psi >_\phi)\, cos(\phi) + \Im(< \bar{\psi}\psi >_\phi)\, sin(\phi)\Big] + i\Big[\frac{1}{2\pi}\underbrace{\int_0^{2\pi} \mathrm{d}\phi \Re(< \bar{\psi}\psi >_\phi)\, sin(\phi) - \Im(< \bar{\psi}\psi >_\phi)\, cos(\phi)}_{0}\Big]$$

An integral $\int_0^{2\pi} \mathrm{d}\phi f(\phi) = 0$ if $f(\phi)$ is an odd function in $\phi$ and periodic in $2\pi$. All terms in the imaginary part of $\Sigma_1'$ are odd and $2\pi$-periodic. This can be seen by taking a close look on (3.17) and (3.18).

$$\Sigma_1' = +\frac{N_c N_f M}{2\pi^3}\int_0^{2\pi} \mathrm{d}\phi \int_0^{\Lambda} \mathrm{dp} \frac{p^2}{E}\left[cos(\phi) + \frac{e^{\beta(E-\mu)}\Big(cos^2(\phi) - sin^2(\phi)\Big) - cos(\phi)}{e^{2\,\beta(E-\mu)} - 2\,e^{\beta(E-\mu)}cos(\phi) + 1} + \frac{e^{\beta(E+\mu)} - cos(\phi)}{e^{2\,\beta(E+\mu)} - 2\,e^{\beta(E+\mu)}cos(\phi) + 1}\right] \tag{3.23}$$

Our approximation for $M$ might have been strong, but we can show that already in this case the dressed Polyakov loop becomes a real parameter, which is something that usually happens in lattice QCD, too.

### 3.2.3 The dressed Polyakov loop for the antiquark

Starting from equation (3.20) we can now calculate $\Sigma'_{-1}$ in a comparable way, which represents the case of the antiquark condensate.

$$\Sigma'_{-1} = -\frac{1}{2\pi}\int_0^{2\pi} \mathrm{d}\phi\, e^{i\phi} < \bar{\psi}\psi >_\phi \tag{3.24}$$

Once again the imaginary part of $\Sigma$ is turning 0.

$$\Sigma'_{-1} = -\frac{1}{2\pi}\int_0^{2\pi} \mathrm{d}\phi(\Re(< \bar{\psi}\psi >_\phi)cos(\phi) - \Im(< \bar{\psi}\psi >_\phi)sin(\phi) - i\underbrace{\left[\frac{1}{2\pi}\int_0^{2\pi} \mathrm{d}\phi(\,\Re(< \bar{\psi}\psi >_\phi)sin(\phi) + \Im(< \bar{\psi}\psi >_\phi)cos(\phi)\right]}_{0} \tag{3.25}$$

$$\Sigma'_{-1} = +\frac{N_c N_f M}{2\pi^3}\int_0^{2\pi} \mathrm{d}\phi \int_0^{\Lambda} \mathrm{d}p \frac{p^2}{E}\left[cos(\phi) + \frac{e^{\beta(E-\mu)} - cos(\phi)}{e^{2\,\beta(E-\mu)} - 2\,e^{\beta(E-\mu)}cos(\phi) + 1} + \frac{e^{\beta(E+\mu)}\left(cos^2(\phi) - sin^2(\phi)\right) - cos(\phi)}{e^{2\,\beta(E+\mu)} - 2\,e^{\beta(E+\mu)}cos(\phi) + 1}\right] \tag{3.26}$$

## 3.3 Comparison between $\Sigma_1$ and $\Sigma_{-1}$

Now it can be seen by comparing eqn. (3.23) and eqn. (3.26) that the difference between $\Sigma'_1$ and $\Sigma'_{-1}$ lies only in the chemical potential

$$\Sigma'_1(-\mu) \;=\; \Sigma'_{-1}(\mu) \tag{3.27}$$

$$\Rightarrow\; \Sigma'_1(\mu = 0) \;=\; \Sigma'_{-1}(\mu = 0) \tag{3.28}$$

As we can see, this also means that for chemical potential $\mu = 0$ the quark and the antiquark condensate must behave equally.

# 4 Numerical Results

## 4.1 The $\phi$-dependent chiral condensate over $\phi$

First of all we want to discuss the boundary condition dependent chiral condensate $< \bar{\psi}\psi >_\phi =: < \sigma >_\phi$. We calculated it in the chiral limit, which means that the current quark mass $m$ is set to zero, and with a small current quark mass ($m = 5.5$ MeV). We will basically follow the calculations of [4] and see besides if we can reproduce the results of that work. From eqn. (3.18) we see that for $\phi = n\pi$, $n \in \mathbb{N}$ the imaginary part of the $\phi$-dependent chiral condensate is zero. For $\phi = \pi$ the $\phi$-dependent chiral condensate returns to be the regular chiral condensate $< \bar{\psi}\psi >_\pi = < \bar{\psi}\psi >$. The constituent mass $M$ has been calculated by solving the gap equation: $M = m - 2G_s < \bar{\psi}\psi >_\phi$, where $m$ is the current quark mass. In order to do so we defined a function

$$f(m, M) = M - m + 2G_s < \sigma >_\phi \tag{4.1}$$

Then we solved $f(m, M_{min}) \stackrel{!}{=} 0$ by using a bisection algorithm. This makes it difficult to calculate an expression for the condensate analytically. For every configuration of $\phi$, T and $\mu$ at first the gap equation needs to be solved. Because of our approximation to assume $M$ to be real we solve this equation in $\mathbb{R}$ only. Even for the calculations for the imaginary part of the condensate.

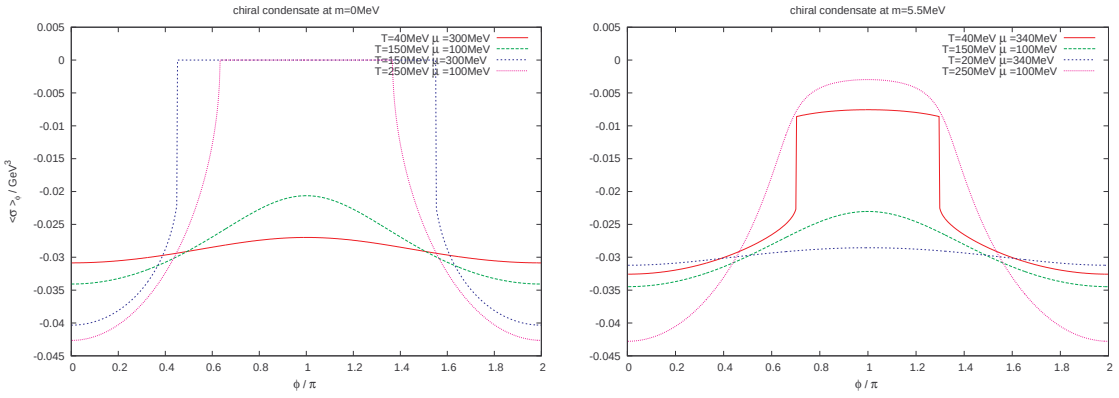


(a) m= 0 MeV (b) m= 5.5 MeV

Figure 4.1: The chiral condensate as a function of $\phi$ with finite bare quark mass m (b) and in the chiral limit (a) at values used in [4]

Figure (4.1) shows behaviour of the $\phi$-dependent chiral condensate for different $\phi$ with configurations for T and $\mu$ as in [4].On the lhs. we see the case of the chiral limit and on the rhs. the behaviour of the condensate for $m = 5.5$ MeV. We can state, that the results from [4] are perfectly reproduced. It is also important to note that the condensate is symetric around $\phi = \pi$ and periodic with $2\pi$ and with that consistent to the expectations from the analytical calculations. For $m = 0$ MeV and $m = 5.5$ MeV $< \sigma >_\phi$ develops a discontinous curve with increasing T and $\mu$.

To get a better understanding of the behaviour of $< \sigma >_\phi$ figure (4.3) shows the results for increasing $\mu$ with a fixed temperature $T = 200$ MeV. Figure (4.2) are the corresponding graphs for constant $\mu = 200$ MeV and variable T.

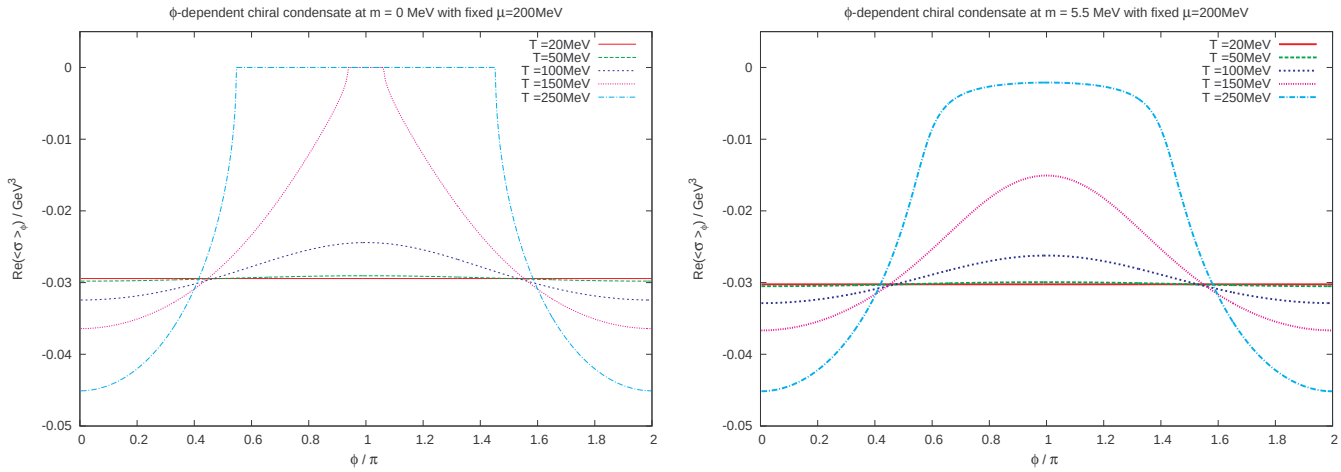


(a) m= 0 MeV (b) m= 5.5 MeV

Figure 4.2: The chiral condensate as a function of $\phi$ at fixed $\mu = 200$ MeV with finite bare quark mass m (b) and in the chiral limit (a)

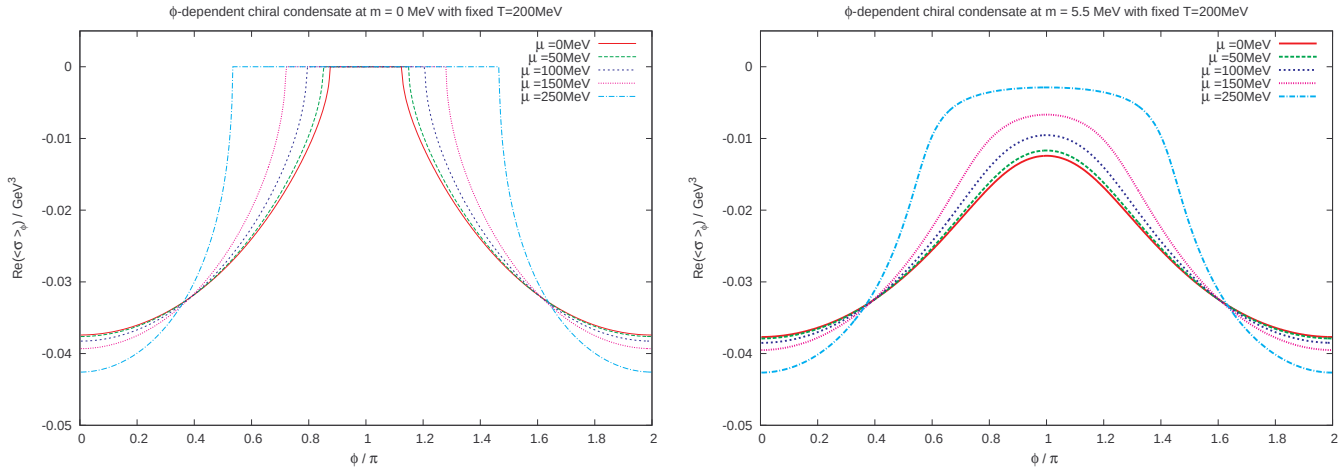


(a) m= 0 MeV (b) m= 5.5 MeV

Figure 4.3: The chiral condensate as a function of $\phi$ at fixed T = 200 MeV with finite bare quark mass m (b) and in the chiral limit (a)

We can see that the $\phi$-dependent chiral condensate is more sensitive to the temperature than to the chemical potential. For small temperatures the fluctuations get very small. For $m = 0$ MeV, $T = 50$ MeV and $\mu = 200$ MeV the difference between the maximal and the minimal value is $\Delta < \sigma >_\phi = 7.5\ \ 10^{-4}$ GeV$^3$.
Increasing the temperature to $T = 250$ MeV gives us a difference of $\Delta < \sigma >_\phi = 0.0451$ GeV$^3$.
Respectively for fixed $\mu = 200$MeV and $T = 50$MeV we have a difference of $\Delta < \sigma >_\phi = 0.037$ GeV$^3$
and for $\mu = 250$ MeV $\Delta < \sigma >_\phi = 0.04258$ GeV$^3$.

In the following figures we take a look at the corresponding imaginary parts of $< \bar{\psi}\psi >_\phi$

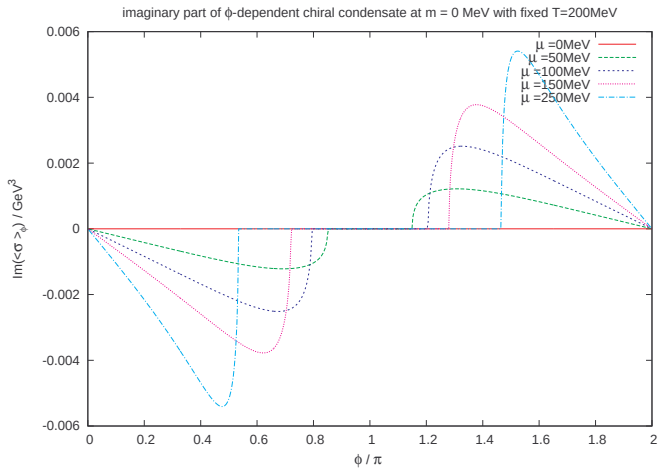


(a) m= 0 MeV

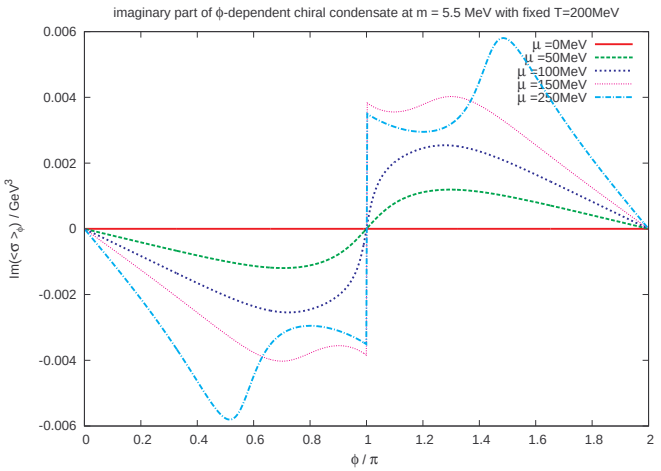


(b) m= 5.5 MeV

Figure 4.4: The imaginary part of the chiral condensate as a function of $\phi$ at fixed T= 200 MeV with finite bare quark mass m (b) and in the chiral limit (a)

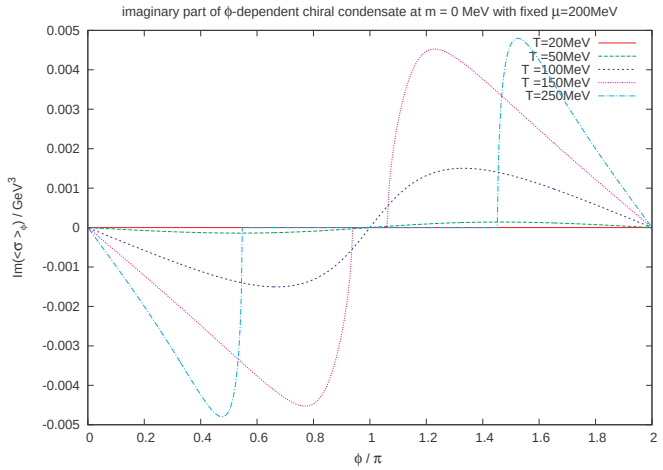


(a) m= 0 MeV

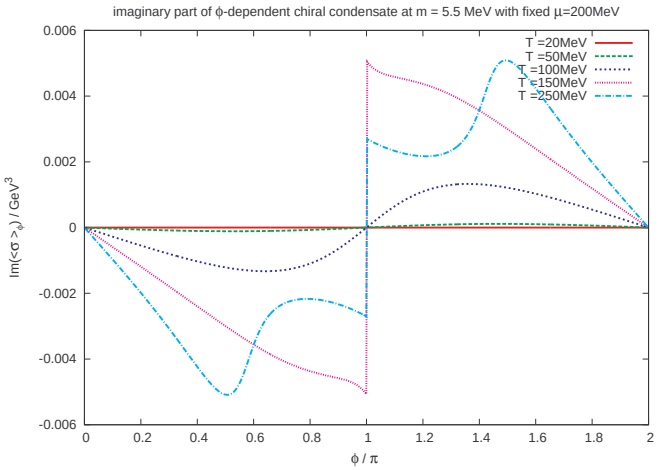


(b) m= 5.5 MeV

Figure 4.5: The imaginary part of the chiral condensate as a function of $\phi$ at fixed $\mu = 200$ MeV with finite bare quark mass m (b) and in the chiral limit (a)

All of the four graphs show an antisymmetric behaviour around $\phi = \pi$. This is consistent with our expectation towards the imaginary part of $< \bar{\psi}\psi >_\phi$ to be an odd function. The imaginary parts do achieve smaller values than the real parts. The maximal values are round about $\frac{1}{10}$ smaller. Thus we can expect, that the behaviour of $\Sigma_1$ can differ from $\Sigma_1'$ but not necessarily in a strong way.

## 4.2 The chiral condensate and the dressed Polyakov loop over T

As previously explained, the NJL model lacks confinement, but it does include the possibility to calculate a chiral condensate and this way a dual condensate. Due to the connection between the dual condensate and the dressed Polyakov loop in QCD it seems worth a shot to calculate it in a comparable way in the NJL model. The analytic background is presented in section (3.2.1). In the following pictures we see the dressed Polyakov loop and the negative chiral condensate with boundary conditions for fermionic fields over the temperature for different values for chemical potential $\mu$. The numerical errors for $\Sigma(\mu = 300$ MeV) were too huge so it was decided not to show these curves.

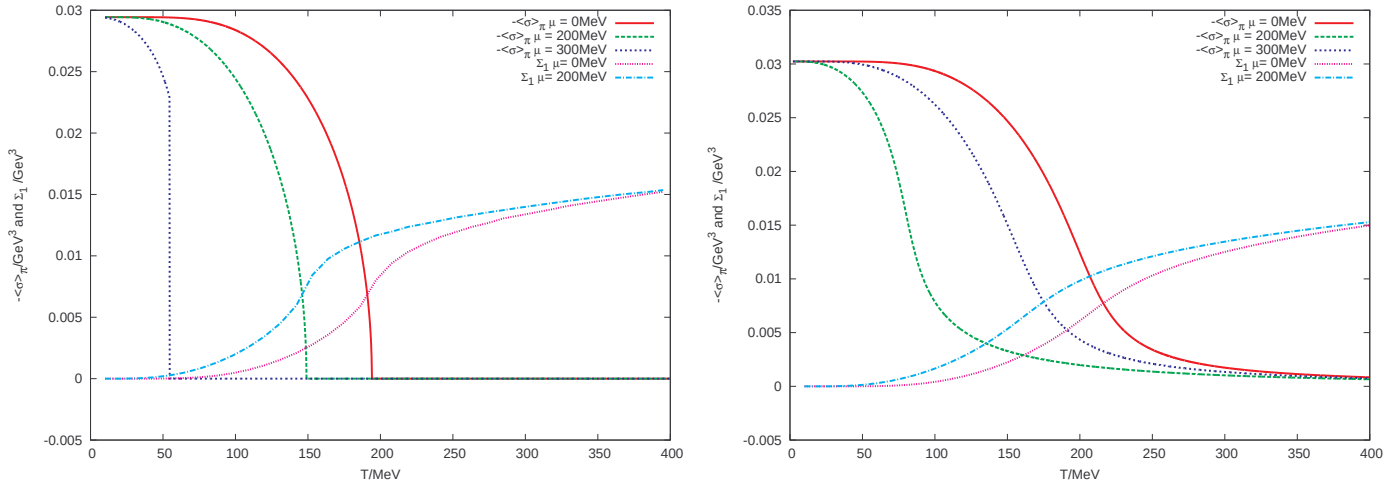


(a) m= 0 MeV (b) m= 5.5 MeV

Figure 4.6: The chiral condensate and the dressed Polyakov loop with finite bare quark mass m (b) and in the chiral limit (a)

The results show that for $m = 0$ MeV there is a strong correspondence between the the inflection point of the dressed Polyakov loop $\Sigma_1$ and the chiral condensate. For $m = 5.5$ MeV the graph shows a shift between these points. $\Sigma_1$ behaves like an order parameter. It is zero for small T, rises with increasing T and saturates in a plateau. The negative chiral condensate does the contrary. It starts at a high plateau, decreases and saturates then to nearly zero for $m = 5.5$ MeV or falls down to zero in the chiral limit. The chiral condensate is already known as an order parameter for chiral symmetry breaking in the NJL-model. The dressed Polyakov loop is known as an order parameter for confinement. As we can see it is possible to calculate a phase transition curve and compare it with the usual chiral phase transition of the of the chiral condensate.

### 4.2.1 Comparison $\Sigma_1$ and $\Sigma_1'$ as functions of T

We calculated the dressed Polyakov loop in two ways, we want to compare $\Sigma_1$ and $\Sigma_1'$ now by calculating them as functions of T for different configurations of $\mu$.

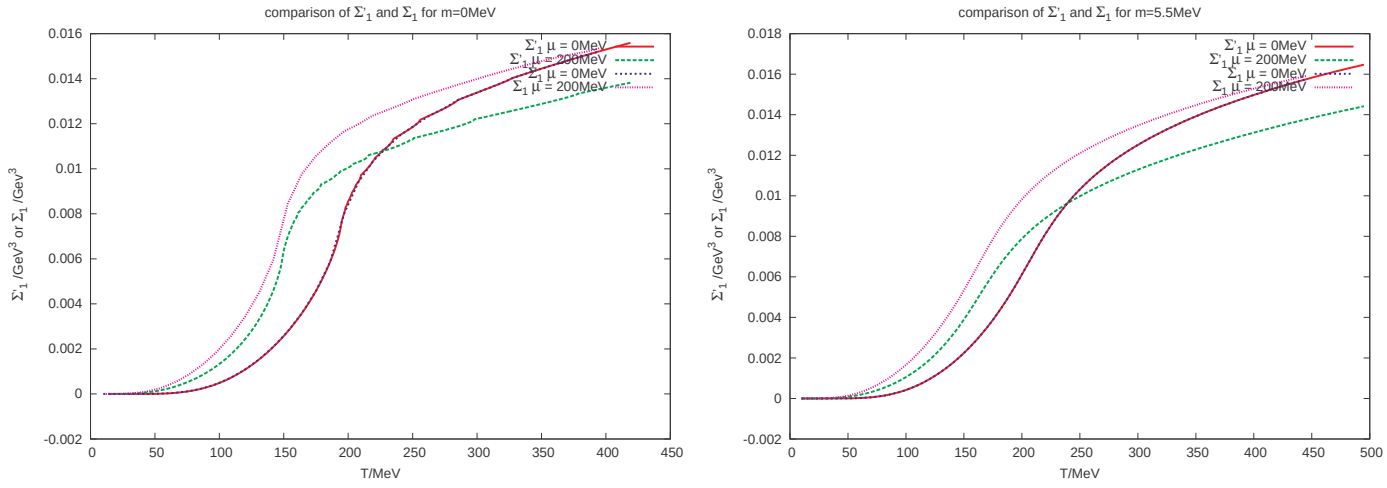


(a) m= 0 MeV (b) m= 5.5 MeV

Figure 4.7: The dressed Polyakov loop with finite bare quark mass m (b) and in the chiral limit (a)

$\Sigma_1$ and $\Sigma_{-1}$ behave equally for $\mu = 0$ MeV. This is no suprise since the imaginary part of $< \bar{\psi}\psi >_\phi$ as seen in eqn.(3.18) or in figure (4.5) and (4.4) turns zero for zero chemical potential. With increasing chemical potential instead $\Sigma_1$ and $\Sigma_1'$ show slightly different behaviour. $\Sigma_1$ increases faster in T than $\Sigma_1'$. From the images it is not decidable, if the position of the inflection is different between the two loop variants. To decide this we have to do a slope analysis.

## 4.3 critical $\mu_c$ and $T_c$

In order to find the inflection points of the order parameters there is used a bisection algorithm onto the second derivative in T-direction. There are other possibilities to calculate the phase transition points like considerating the derivative in $\mu$ direction. As we already saw, $< \sigma >_\phi$ varies strongly in T, so our way is a plausible choice. It was possible to reproduce most of the parts presented in [4].

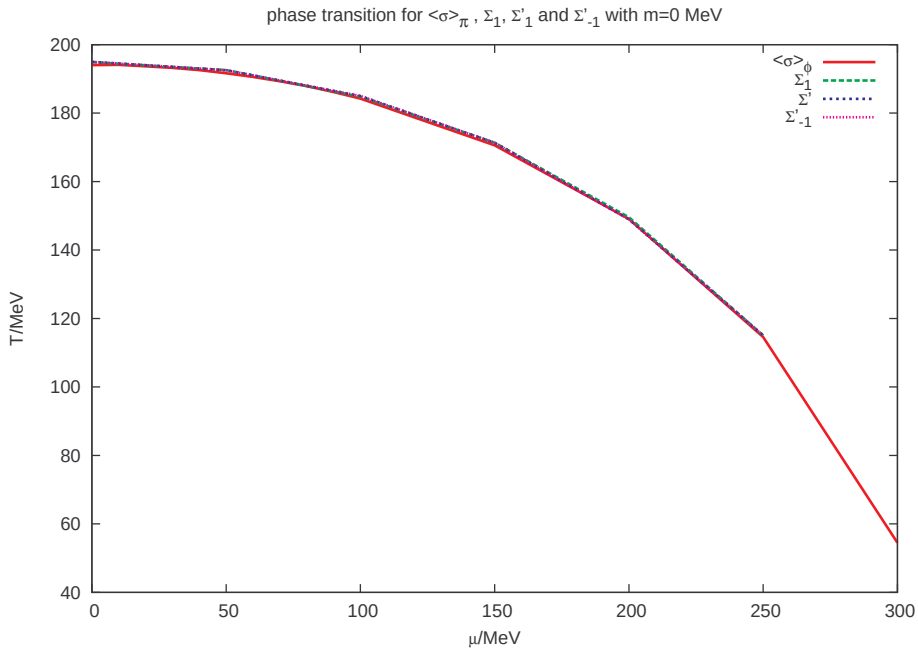


Figure 4.8: The phase transition for m=0 MeV

In fig. (4.8) the results for $\Sigma_1$, $\Sigma_{-1}'$ and $\Sigma_1'$ for $\mu > 250$MeV are not sufficently accurate. Apart from that area the calculations show that the Polyakov loops, the values for the antiquark and the chiral condensate coincide in the chiral limit.

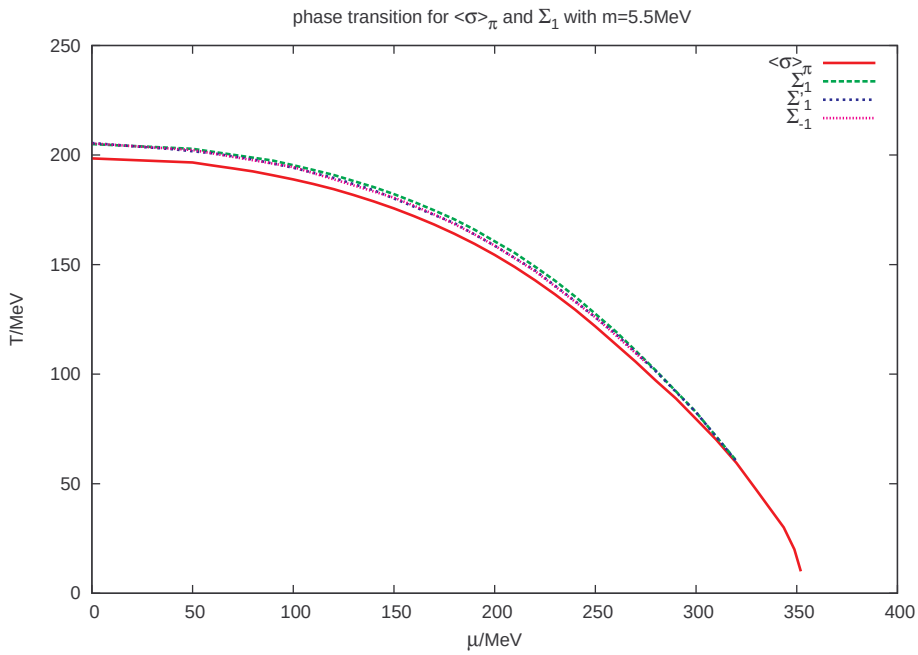


Figure 4.9: The phase transition for m=5.5 MeV

In figure (4.9) this happens to the results for the dressed polyakov loops at $\mu > 325$ MeV. So it was not possible to reproduce these parts of [4]. This is by now clearly a numerical problem. The chiral condensate show at m=5.5 MeV and T<20 MeV in $\mu$ direction a behaviour like a first order phase transition. The graphs show definitely that in chiral limit the chiral symmetry transition and the confinement transition conditions are fullfilled at same $(T, \mu)$ and for $m = 5.5$ MeV the graphs seperate with decreasing chemical potential. We also see that $\Sigma_1'$ behaves quite comparable to $\Sigma_1$ but they do not behave equally. The graphs for $\Sigma_1'$ and $\Sigma_{-1}'$ behave equally, which means that both show transition parameter behaviour at the same sets of T and $\mu$. With increasing $\mu$ the difference of the transition temperatures between the loops increases and decreases again to finally arrive at the same point as the transition values for the chiral condensate and $\Sigma_1$ Consequently it is possible to compare the correspondence of the crossover behaviour for both symmetries for different $m$.

## 4.4 Correspondence between $\sigma_1$ and $< \sigma >_\phi$ for different m

In the previous section we saw that the transition temperatures for the dressed Polyakov loop and the chiral condensate are equal in the chiral limit, but differ in the case of a small bare quark mass $m = 5.5$ MeV. So we would like to compare the transition temperatures for both order parameters. $\Sigma_1'$ we do not have to consider, since we already saw several times that there is no difference between $\Sigma_1$ and $\Sigma_1'$ for $\mu = 0$ MeV.

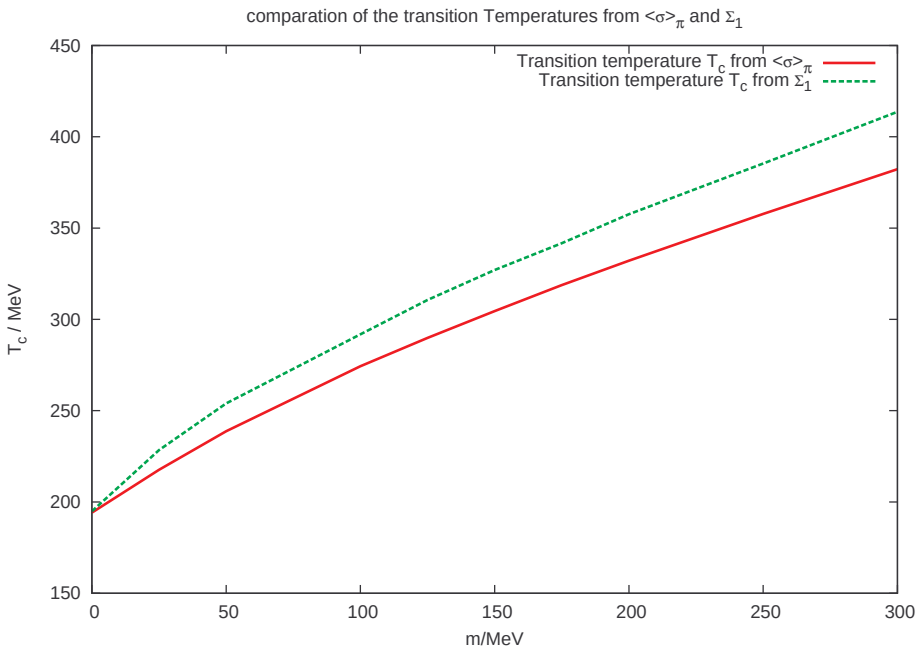


Figure 4.10: The phase transition for $\mu = 0$MeV as a funcition of m

The difference between the transition values increases with the bare quark mass $m$. This shows us the limits of the dressed polyakov loop as it is used in this theory, that is a confinement transition parameter.

## 5 Conclusion and outlook

In this work we calculated the dressed Polyakov loop, normally an order parameter for confinement in the NJL model, a model without confinement to compare the transition behaviour of the dressed Polyakov loop with the transition behaviour of the chiral condensate, an order parameter for chiral symmetrie breaking. In QCD it is found, that for zero chemical potential the transition temperatures can be near to each other. We saw, that in the chiral limit the dressed polyakov loop and the chiral condensate show the same phase transition curves and for small bare quark mass they behave similar with smaller chiral transition temperatures than confinement transition temperatures. This can mean, that in the way which the dressed Polyakov loop is calculated here, could be a way to do calculations concerning confinement.
There were two ways presented here to calculate the dressed Polyakov loop. Both with strong approximations. For the next step it could be of interest, if we get comparable results, assuming the constituent mass $M$ to be complex.

## Bibliography


[1] Erek Bilgici; *Signatures of confinement and chiral symmetry breaking in spectral quantities of lattice Dirac operators*; Ph.D. thesis; Karl–Franzens–Universität Graz; 2009.

[2] Michael Buballa; *NJL-model analysis of dense quark matter.*; Phys Rep; **volume 407**: 205; 2005.

[3] J. I. Kapusta and C. Gale; *Finite-Temperature Field Theory*; Cambridge University Press; second edition edition; 2006.

[4] Tamal K. Mukherjee, Huan Chen, and Mei Huang; *Chiral condensate and dressed Polyakov loop in the Nambu-Jona-Lasinio model*; Phys Rev D; **volume 82**: 034015; 2010.

[5] Y. Nambu and G. Jona-Laisinio; *Dynamical Model of Elementary Particles Based on an Analogy with Superconductivity*; Physical Review; **volume 122**, 1: 346; 1961.